Development 135, 281-290 (2008) doi:10.1242/dev.011494

Maternal-zygotic medaka mutants for *fgfr1* reveal its essential role in the migration of the axial mesoderm but not the lateral mesoderm

Atsuko Shimada[1,*,†], Mina Yabusaki[1,*], Hitomi Niwa[1,*], Hayato Yokoi[1,‡], Kohei Hatta[2], Daisuke Kobayashi[1] and Hiroyuki Takeda[1,†]

The medaka fish (*Oryzias latipes*) is an emerging model organism for which a variety of unique developmental mutants have now been generated. Our recent mutagenesis screening of the medaka identified *headfish* (*hdf*), a null mutant for *fgf receptor 1* (*fgfr1*), which fails to develop structures in the trunk and tail. Despite its crucial role in early development, the functions of Fgfr1-mediated signaling have not yet been well characterized due to the complexity of the underlying ligand-receptor interactions. In our present study, we further elucidate the roles of this pathway in the medaka using the *hdf* (*fgfr1*) mutant. Because Fgfr1 is maternally supplied in fish, we first generated maternal-zygotic (MZ) mutants by transplanting homozygous *hdf* germ cells into sterile interspecific hybrids. Interestingly, the host hybrid fish recovered their fertility and produced donor-derived mutant progeny. The resulting MZ mutants also exhibited severe defects in their anterior head structures that are never observed in the corresponding zygotic mutants. A series of detailed analyses subsequently revealed that Fgfr1 is required for the anterior migration of the axial mesoderm, particularly the prechordal plate, in a cell-autonomous manner, but is not required for convergence movement of the lateral mesoderm. Furthermore, *fgfr1* was found to be dispensable for initial mesoderm induction. The MZ *hdf* medaka mutant was thus found to be a valuable model system to analyze the precise role of *fgfr1*-mediated signaling in vertebrate early development.

KEY WORDS: Medaka, *fgfr1*, Mesoderm, Prechordal plate, Hybrid sterility

INTRODUCTION

The medaka fish, *Oryzias latipes*, is a model vertebrate that has generated increasing interest in both developmental and evolutionary biology (Ishikawa, 2000; Naruse et al., 2004; Wittbrodt et al., 2002). In addition to the recent completion of the medaka draft genome (Kasahara et al., 2007), large-scale mutational screens using this organism have identified a number of genetic loci that are required for normal embryonic development (Furutani-Seiki et al., 2004). Some medaka mutations also appear to be unique, ensuring that the medaka and zebrafish are complementary model systems. Indeed, in our recent mutagenesis screening, we isolated the medaka *headfish* (*hdf*) mutant showing a severe defect in trunk-tail development, which is a phenotype that has not so far been identified in zebrafish. Our subsequent analysis revealed that this *hdf* mutant harbors a tryptophan-to-cysteine substitution at a highly conserved amino acid position in the extracellular Ig-like domain II (the ligand-binding domain) of *fgf receptor 1* (*fgfr1*), and is therefore the first *fgf-receptor*-related null mutant so far described in fish (Yokoi et al., 2007).

The gene *fgf receptor* encodes a cell surface tyrosine kinase receptor that binds extracellular Fgfs and transduces the resulting signals into the cytosol (Bottcher and Niehrs, 2005). Among the four Fgf receptor genes that have been characterized, *fgfr1* is thought to play a crucial role in early vertebrate development, but its precise function has yet to be elucidated due to the promiscuity of the Fgf receptor family and the large number of possible ligands. In amphibians and teleosts, functional analyses of *fgfr1* have mainly been performed by injection of RNA molecules encoding dominant-negative forms of Fgfr1 (XFD) (Amaya et al., 1991; Amaya et al., 1993; Carl and Wittbrodt, 1999; Griffin et al., 1995; Launay et al., 1996), but this inevitably interferes with each of the Fgfr family members (Ueno et al., 1992).

We previously reported that this *hdf* (*fgfr1*) mutant exhibits a severe trunk-tail truncation with relatively normal head structures (Yokoi et al., 2007). However, this phenotype seemed less severe than expected, because both mesoderm induction and neural patterning are known to depend upon Fgf signaling in fish (Thisse and Thisse, 2005). This may be due to the presence of other Fgfr species or maternally supplied Fgfr1. Indeed, the ubiquitous expression of *fgfr1* is detected in medaka embryos from early cleavage (four-cell) to early gastrula stages (Yokoi et al., 2007). As gastrulation proceeds, *fgfr1* expression is increased in the dorsal margin, the presumptive anterior neural region and the underlying hypoblast (Yokoi et al., 2007). Furthermore, *fgfr4* is also expressed during early gastrula, while *fgfr2* and *fgfr3* begin to express from late gastrula stages (H.Y., unpublished). To distinguish between genetic redundancy and maternal effect, we have analyzed the function of Fgfr1 in mutant embryos in our present study, in which both maternally and zygotically loaded gene products are eliminated, i.e. maternal-zygotic (MZ) mutants.

As functional gene products are usually generated by a wild-type allele of a heterozygous germ cell during oogenesis, the simplest way to obtain MZ mutant embryos is to replace the wild-type host germ cells with the corresponding homozygous mutants. Indeed, Schier and colleagues recently reported the production of MZ mutant zebrafish by transplantation of mutant germ cells into host

[1]Department of Biological Sciences, Graduate School of Science, University of Tokyo, Bunkyo-ku, Tokyo, Japan. [2]Graduate School of Life Science, University of Hyogo, 3-2-1 Kouto, Kamigori, Ako-gun, Hyogo 678-1297, Japan.

*These authors contributed equally to this work
†Authors for correspondence (e-mails: kirita@biol.s.u-tokyo.ac.jp; htakeda@biol.s.u-tokyo.ac.jp)
‡Present address: Institute of Neuroscience, University of Oregon, Eugene, OR, USA

Accepted 15 October 2007

embryos in which the endogenous germ cells had first been eliminated by the morpholino-knockdown of the essential gene, *dead end* (Ciruna et al., 2002). In our current study, we utilize both this morpholino-knockdown method and a novel method that we have ourselves developed for the production of MZ medaka mutants using interspecific hybrids as the host embryos.

Interspecific hybrids are generally sterile (i.e. hybrid sterility) and this is also the case for medaka. Among the several species that are closely related to the genus *Oryzias*, the hybrid offspring from the Japanese medaka (*O. latipes*) and Chinese Hainan medaka (*O. curvinotus*) appeared to be healthy, although all are sterile as their gonads are sexually differentiated but have severely impaired oogenesis and spermatogenesis (Hamaguchi and Sakaizumi, 1992). Taking advantage of these characteristics, we have developed a new method of germline replacement in which these hybrids are used as a host for the production of MZ mutant offspring.

We herein report for the first time a detailed phenotypic analysis of medaka MZ mutants and reveal unexpected early roles for *fgfr1* in fish development. We find that *fgfr1*-mediated signaling plays an essential role in the expansion and anterior migration of the axial mesoderm. By contrast, this signaling is not required for the dorsal convergence of the lateral mesoderm, and Fgfr1 is even dispensable for mesoderm induction in fish.

MATERIALS AND METHODS

Generation of hybrid fish embryos for germ-cell replacement

Interspecific hybrid embryos were obtained by natural matings between the Kaga inbred strain derived from the Japanese northern population and the Chinese Hainan medaka. The Hainan medaka was collected in Hong Kong, China, by Dr Hirohi Uwa, and has since been bred at Shinshu University and at the Niigata University. The *hdf* (*fgfr1*) mutant medaka originated from the d-rR strain whose genetic background is the Japanese southern population.

Cell transplantation experiments

Donor embryos were injected at the one-cell stage with 1.65% lysine fixable tetramethylrhodamine-dextran (10 kDa; Molecular Probes). At the morula stage, both the donors and hosts were dechorionated by hatching liquid (Yasumasu et al., 1989). At the mid-blastula stage [for primordial germ cell (PGC) transplantation], or at the shield stage (for shield transplantation), the embryos were placed on V-shaped grooves of a 1.5% agarose gel immersed in Yamamoto's Ringer's solution (Yamamoto, 1956), and then the cells were transplanted using a micromanipulator (Narishige M-152) in combination with a microinjector (Narishige IM-6).

Genotyping of donor embryos

Donor embryos were fixed with 100% ethanol just after transplantation. Genomic DNA was then extracted using a QIAamp DNA Micro Kit (Qiagen). Genomic DNA fragments corresponding to the site of the mutation point were amplified using the primer set F: 5′-GGAATGTACC-CAAGTGTGAAAG and R: 5′-AGAAGAGAGACCCATGCCAC. The immunoglobulin II domain region of the *fgfr1* gene, including the G→C mutation site, was sequenced using the Dynamic ET Terminator Cycle Sequencing Kit.

Whole-mount in situ hybridization

Embryos were fixed with 4% paraformaldehyde (PFA)/PBS overnight at room temperature. Hybridization was performed with DIG-labeled RNA probes at 65°C overnight. Signals were detected by alkaline-phosphate (AP)-conjugated anti-DIG Fab fragments (1:8000) and BM Purple (Boehringer Mannheim).

Histological analysis

Ovaries were dissected, fixed in Bouin's solution and embedded in paraffin. The specimens were then sectioned at 5 μm and stained with Hematoxylin. For embryos, embedding was performed with a Technovit 8100 (Heraeus Kulzer, Wehrheim).

Cell-tracing experiments

Two per cent DMNB-caged fluorescein-dextran (molecular weight 10,000, Molecular Probes) was injected into the cytoplasm of one-cell-stage embryos, which were then grown in the dark until the shield stage. To uncage the dye, a beam of ultraviolet light, generated using a DAPI filter set, was directed for 5 seconds at the dorsal or lateral blastoderm margin. The locations of the cells containing uncaged fluorescein-dextran were monitored and recorded at the indicated periods. Images were quantitatively analyzed using NIH image J.

RESULTS

Production of MZ mutants for *hdf* (*fgfr1*)

The *hdf* mutant is embryonic lethal and homozygous adult fish producing maternally depleted eggs are thus not available. We therefore generated MZ embryos by replacing the wild-type host germ cells with homozygous mutants. To this end, we explored a new approach to achieving germline replacement, which is depicted in Fig. 1. As the host, we prepared interspecific hybrids of Japanese medaka, Kaga and Chinese Hainan medaka embryos (Fig. 2A,B). These interspecific hybrids grow well to adulthood but do not subsequently produce any normal eggs or sperm that can be fertilized (Hamaguchi and Sakaizumi, 1992).

We first validated our method by transplanting cells from a wild-type orange-red strain. Donor medaka embryos were injected at the one-cell stage with rhodamine-dextran and the resulting blastula stage cells were then transplanted from the deep layer of the blastoderm, where medaka PGCs tend to reside (Kurokawa et al., 2006), into the animal pole of the hybrid hosts. Transplanted donor cells include both somatic cells and PGCs, which segregate during early development. The former cells contribute to the anterior neural ectoderm, whereas some of the latter reached the gonadal region. The successful transfer of donor PGCs was thus assessed by the presence of rhodamine-dextran-labeled cells in the gonadal mesoderm at the segmentation stages (52/174) (Fig. 2C). The host embryos that had been successfully transplanted were subsequently selected and raised to adulthood (Fig. 2D,E).

Among the 20 females initially produced using this technique, 12 recovered their fertility and produced donor-derived eggs. Histological sections also revealed that the hybrid ovaries that had been transplanted with normal PGCs contained both normally growing oocytes, possibly from the donor, and impaired hybrid tissues (Fig. 2I-K). The orange-red donor strain (*b*/*b*) lacks melanophores, which are present in the skin of the hybrid host (*B*/*B*) (Fukamachi et al., 2001). Thus, we could confirm a successful germline replacement by determining the presence of melanophores in the skin of the progeny (Fig. 2F-H). Further confirmation was obtained by analysis using genetic markers that can discriminate between each strain via PCR-length polymorphisms (Kimura et al., 2004) (Fig. 2L).

We next transplanted germ cells derived from heterozygous *hdf* (*fgfr1*) parents. For the first five fertile host females, we retrospectively genotyped their donor embryos by sequencing an appropriate region of the *fgfr1* gene. One donor embryo was genotyped as wild type (+/+), two as heterozygous (+/–) and two as homozygous (–/–). The two hybrid hosts transplanted with these homozygous PGCs eventually produced MZ offspring. In a later series of experiments, the donor embryos were allowed to develop further and their genotype was determined by an assessment of their external morphology.

In addition to our novel method, we also obtained MZ mutants using a conventional knockdown method (Ciruna et al., 2002) in which the host germ cells are eliminated by the morpholino-

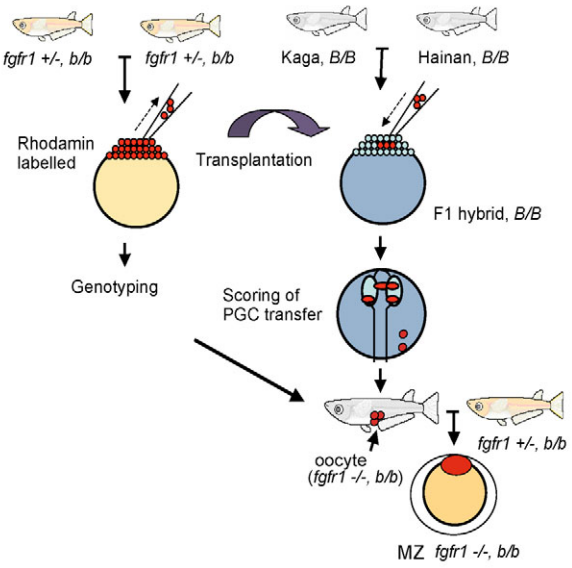

Fig. 1. Schematic representation of the production of an MZ hdf (*fgfr1*) medaka mutant by germline replacement.

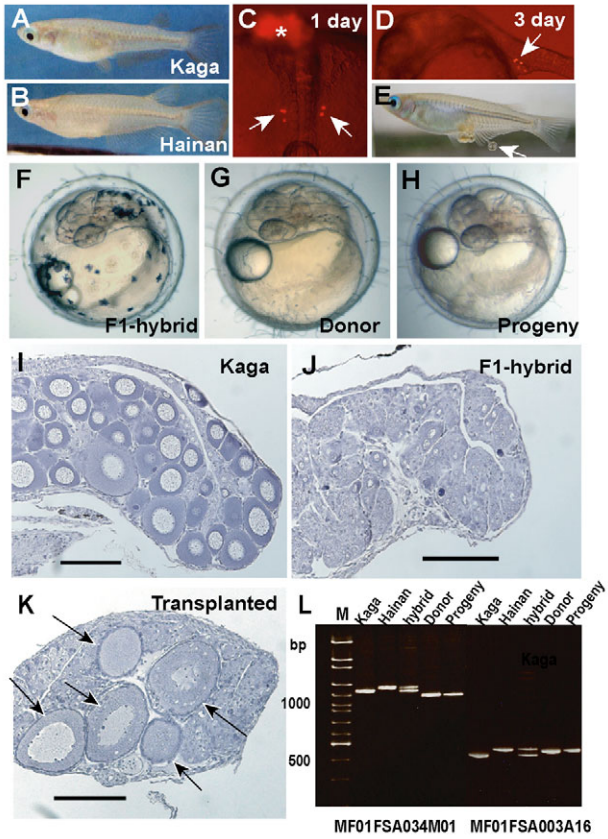

Fig. 2. Development and transfer of a donor germline into a hybrid host. (**A**,**B**) Parental strains used for the production of interspecific medaka hybrids. (A) A Kaga female. (B) A Hainan male. (**C**,**D**) A chimeric host embryo at 1 day (four-somite stage) (C) and 3 days (D) post-fertilization showing a successful transfer of donor PGCs (arrows). The somatic contribution of the donor cells to the anterior neuroectoderm lineage is also shown (* in C). (**E**) A representative matured host female with a cluster of fertilized eggs (arrow). (**F-H**) Confirmation of a successful germline transfer by detection of the pigmentation marker gene, *b*. (F) F1-hybrid; *B/B*. (G) Donor; *b/b*. (H) Progeny of a transplanted hybrid host female; *b/b*. The embryos shown are at 2 days post-fertilization. (**I-K**) Cross sections of ovaries from a 4-week-old Kaga strain (H), non-transplanted hybrid (J) and transplanted F1-hybrid host (K). The transplanted hybrid ovary contains growing oocytes (arrows in K). (**L**) Confirmation of germline transfer by detection of strain-specific genetic markers. Two M-markers (Kimura et al., 2004) were amplified from genomic DNAs of Kaga, Hainan, F1-hybrid, donor and the progeny of the F1-hybrid transplanted with donor PGCs. Note that the patterns of marker amplification for the progeny are identical to those of the donor. Scale bars: 200 μm.

knockdown of *cxcr4*, an essential gene for directing PGC migration toward the gonads (Kurokawa et al., 2006). The phenotypes of the MZ mutants obtained using these two methods were found to be indistinguishable (data not shown). This indicates that the environment of the hybrid host does not affect the later development of their progeny, thus validating our new germline replacement strategy.

Gross morphology of the MZ *hdf* (*fgfr1*) mutant

The MZ mutant for *hdf* (*fgfr1*) exhibited a far more severe phenotype than its zygotic mutant counterpart, indicating that the maternal contribution of Fgfr1 plays a significant role during early development in fish. In this regard, the significant phenotypic abnormalities associated with the MZ *hdf* mutant embryo included a severe truncation of trunk (compare Fig. 3B with D, also F with H). Furthermore, the development of the anterior head structures was impaired in this MZ mutant embryo, but was never observed in the corresponding zygotic mutant (compare Fig. 3B with D, also F with H). When examined during the segmentation stages [6-somite (st. 21) to 30-somite (st. 28)], an anterior phenotype became evident in the MZ mutants, with the most severe cases displaying complete cyclopia (Fig. 3U). Cross sections at various levels of anterior regions further revealed the morphological abnormalities of the MZ *hdf* mutant, including fused retina (arrow in Fig. 3L), abnormally formed large midbrain (arrow in Fig. 3P) and hindbrain (arrow in Fig. 3T). Furthermore, we frequently observed that mesenchymal cells were abnormally accumulated at the level of the midbrain to hindbrain (asterisks in Fig. 3P,T; see also Fig. 8R in the transplantation experiment). Intriguingly, the maternal –/–; zygotic +/– embryos (referred to as maternal or M mutants) developed normally (Fig. 3C,G,K,O,S), indicating that zygotically supplied Fgfr1 can compensate for the lack of maternal Fgfr1.

Fgfr1-mediated signaling is not required for mesoderm induction

We first examined whether the mesoderm is initially formed in the MZ *hdf* (*fgfr1*) mutant. In the medaka wild-type embryo, the expression of the pan-mesoderm marker *no tail* (*ntl*) is initiated in the blastoderm margin during the late blastula to early gastrula stages (Fig. 4A). During these stages we cannot genotype these embryos using their external morphology, but *ntl* expression remained detectable in all embryos obtained using any combination of parental crosses (Fig. 4A-D). However, the levels of *ntl* expression, particularly in the dorsal margin (fated to become the organizer, arrows in Fig. 4A-D), were reduced in the embryos that were thought to be zygotic or MZ mutants (Fig. 4B,D). A similar tendency was also observed with another early mesoderm marker, *fgf8* (Fig. 4E-H), as well as with the dorsal mesoderm marker *chordin* (Fig. 4I-L).

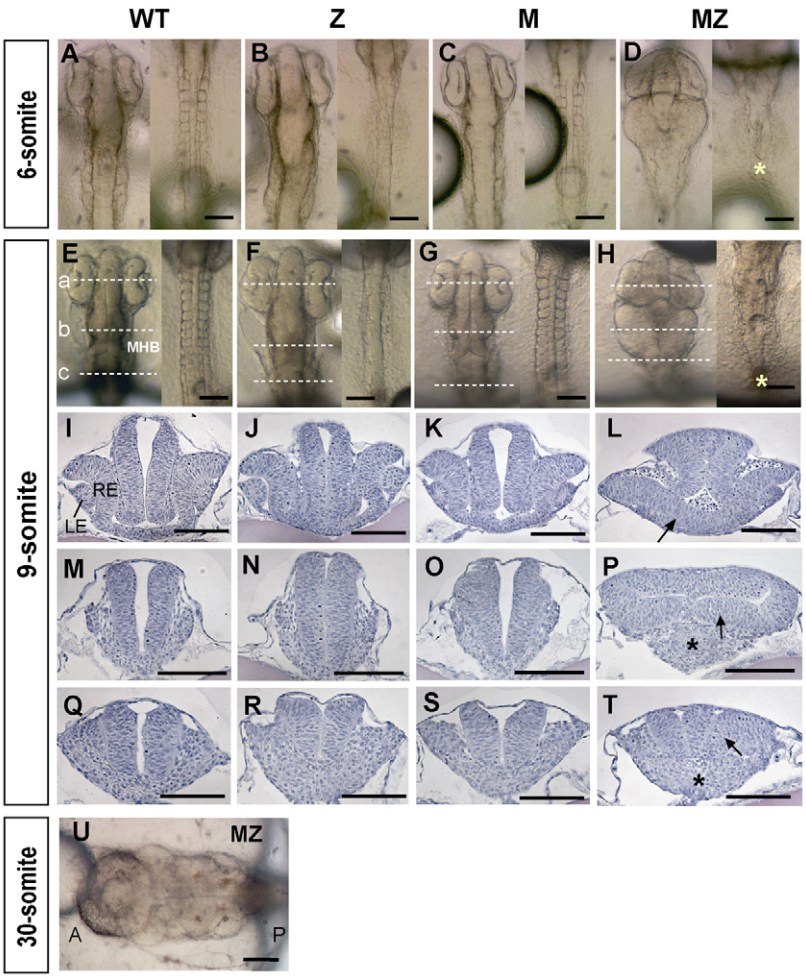

Fig. 3. Gross morphology of the *hdf* (*fgfr1*) mutants at segmentation stages. (**A-H**) Dorsal views of the head (left) and trunk (right) regions at the six-somite stage (st. 21) (A-D) and nine-somite stage (st.22) (E-H). Asterisks in D and H indicate posterior limits of the trunk. (**I-T**) Cross sections at the levels of forebrain (I-L), midbrain (M-P) and hindbrain (Q-T) indicated by the dashed lines, a-c in E-H, respectively. (**U**) A dorsal view of the anterior head of the MZ embryo at the 30-somite stage. The anterior head structures are relatively normal in the zygotic (B,F,J,N,R) and maternal (C,G,K,O,S) mutants, although the head in the zygotic mutant is slightly larger than wild type (A,E,I,M,Q). By contrast, in the MZ mutant the brains display abnormal morphologies with a cyclops appearance (D,H,U and arrow in L), large and flattend midbrain (D,H, and arrow in P) and extra hindbrain (arrow in T). Note that mesenchymal cells are abnormally accumulated at the level of the midbrain to hindbrain (asterisks in P and T). Scale bars: 100 μm. A, anterior; LE, lens; M, maternal; MHB, midbrain-hindbrain boundary; MZ, maternal-zygotic mutants; P, posterior; RE, retina; WT, wild type; Z, zygotic.

We next examined the expression levels of *sprouty4*, a downstream target of Fgf signaling, in the margins of the embryos obtained by identical parental crosses. Approximately 50% of the hybrid host progeny with mutant germ cells (considered to be M mutants) exhibited almost normal levels of *sprouty4* expression (Fig. 4O), whereas this expression was found to be undetectable in the remaining 50% (considered to be MZ mutants) (Fig. 4P). We also detected slight expression of *sprouty4* in approximately 25% of the embryos derived from heterozygous *hdf* parents [considered to be zygotic (Z) mutants] (arrowheads in Fig. 4N), suggesting that maternal Fgfr1 is functional by at least this early gastrula stage. Hence, the early mesodermal markers appear to be activated without detectable levels of *sprouty4* expression in the MZ mutant embryo. From these data, we reasonably contend that Fgfr1-mediated signaling is not required for initial mesoderm induction and its dorsoventral patterning in the medaka embryo.

In the MZ mutant, we speculated that other members of the Fgfr family might mediate the mesoderm induction process. To examine this possibility, we treated wild-type embryos with different concentrations of SU5402, a chemical inhibitor of nearly all types of Fgfrs (Mohammadi et al., 1997). The embryos were incubated in the presence of SU5402 from the 32- to 64-cell to early gastrula stages, and immediately subjected to in situ hybridization with *ntl* or *sprouty4* probes. As shown in Fig. 4Q-S, the levels of *ntl* expression were slightly reduced with increasing concentrations of SU5402, but persisted at the 0.1 mg/ml concentration. By contrast, *sprouty4* expression was greatly reduced or undetectable at the 0.05 or 0.1 mg/ml concentrations, respectively (Fig. 4T-V). SU5402 exposure at a higher concentration than 0.1 mg/ml was found to cause a profound toxic effect on the entire development of embryos and is therefore not likely to give a physiological response (data not shown). These results further support the idea that the mesoderm is initially formed in the absence of Fgf signaling.

Expression analysis of anterior neural markers in the MZ *hdf* (*fgfr1*) mutant

We next examined the anterior neural patterning in wild-type, zygotic, maternal and MZ *hdf* (*fgfr1*) mutant embryos at the bud (st. 18) and 12-somite (st. 23) stages. The markers used were *krox20* for rhombomere 3 and 5, *pax2* for the MHB, and *bf1* for the telencephalon (Fig. 5A,E). *Krox20* expression in rhombomere 5 was found to be affected in all of the mutants at the bud stage (Fig. 5A-D). *Pax2* expression in the midbrain-hindbrain boundary (MHB) was activated in all of the mutant types at the bud stage (Fig. 5A-D). In the MZ mutant, however, *pax2* expression was found to decrease by the 12-somite stage (red arrow in Fig. 5H) and to have disappeared by the 16-somite stage (data not shown), whereas this expression was maintained in both the zygotic and maternal mutants (red arrows in Fig. 5F,G). The expression domain of *bf1* was normal in the zygotic and maternal mutants, but smaller in size in the MZ mutant (black arrow in Fig. 5H). Furthermore, *fgf8* (data not shown) and *sprouty4* were expressed in the anterior telencephalon and MHB in each type of mutant at the bud stage (Fig. 5I-L). At the 12-somite stage, however, the expression of these two genes, particularly in the

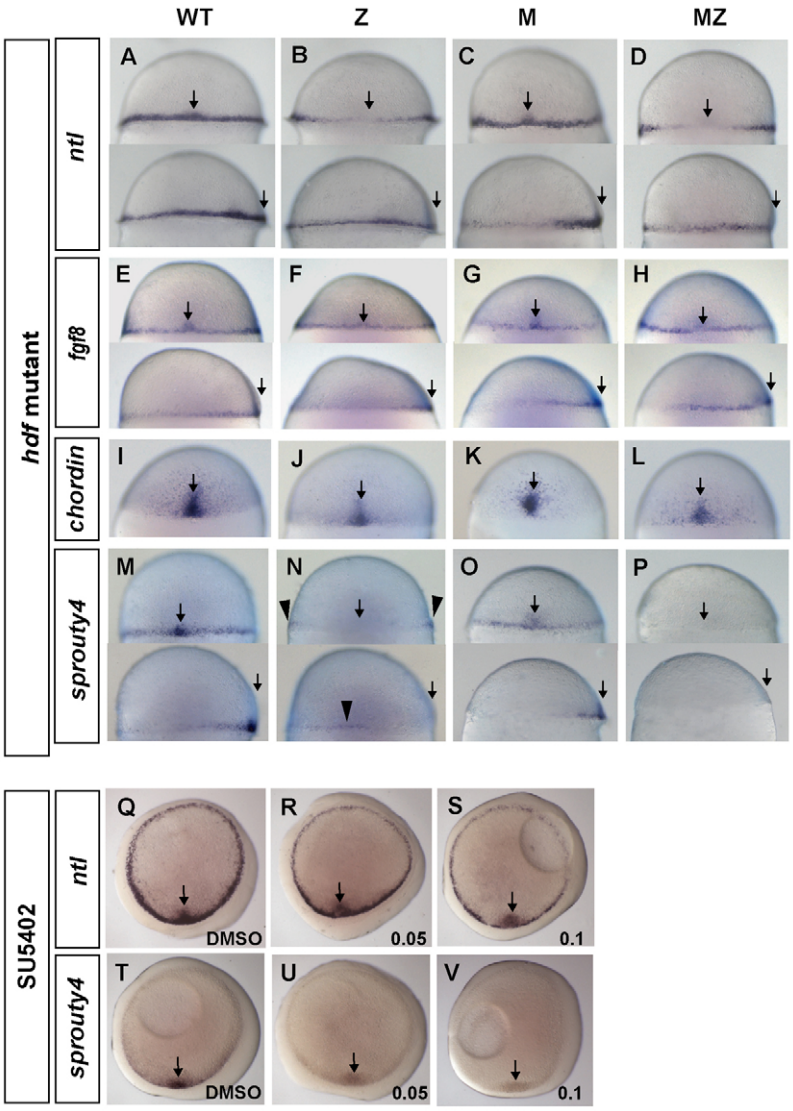

Fig. 4. Mesoderm induction in the MZ *hdf* (*fgfr1*) medaka mutant. (**A-P**) Expression of the early mesoderm markers, *no tail* (*ntl*) (A-D) and *fgf8* (E-H), dorsal mesoderm marker, *chordin* (I-L), and the Fgf-downstream target, *sprouty4* (M-P), in each of the indicated types of *hdf* (*fgfr1*) mutant at the early gastrula stage (50% epiboly, st. 15). Dorsal (upper) and lateral (lower) views of the same embryo are shown in A-D, E-H and M-P. Arrows indicate the organizer region; arrowheads in N indicate weak expression of *sprouty4*. The embryos of each genotype express *ntl* (A-D), *fgf8* (E-H) and *chordin* (I-L) in the blastoderm margin. (**Q-V**) *ntl* and *sprouty4* expression in SU5402-treated embryos at the early gastrula stage (50% epiboly, st. 15). Embryos were treated with SU5402 at concentrations of 0 (2% DMSO) (Q,T), 0.05 (R,U), and 0.1 mg/ml (S,V) from morula to 50% epiboly. The level of *ntl* expression persisted at the 0.1 mg/ml concentration, whereas *sprouty4* expression was undetectable. M; maternal; MZ; maternal zygotic *fgfr1* mutants; WT, wild type; Z, zygotic.

MHB region, became reduced or undetectable only in the MZ mutant (Fig. 5M-P). Taken together, these data show that in the MZ mutant, the forebrain and MHB structures are formed but are not well maintained at later developmental stages, whereas the anterior head patterning proceeds normally in both the zygotic and maternal mutants.

Development of the prechordal plate is impaired in the MZ *hdf* (*fgfr1*) mutant

Cyclopia and abnormal development of the forebrain and MHB are sometimes observed when the underlying axial mesoderm, or the prechordal plate, fails to develop normally (Fekany et al., 1999; Schier et al., 1997; Shinya et al., 2000). This prompted us to examine the expression of *goosecoid* (*gsc*) in the prechordal plate in each of our *hdf* (*fgfr1*) mutant types at the bud stage (Fig. 6). The prechordal plate is a group of cells that first involutes under the epiblast in the blastoderm margin, then moves anteriorly and finally passes over the anterior end of the neural plate (anterior neural ridge), reaching near to the animal pole (Fig. 6A). As judged by the *gsc* expression profile, this anterior limit of the prechordal plate is posteriorly shifted in the MZ mutant embryos (Fig. 6D). However, neither the zygotic nor maternal *hdf* mutants show these phenotypes (Fig. 6B,C). The severity of the anterior neural phenotype in the MZ mutant was found to correlate with the extent to which the prechordal plate underlies the anterior neural region (data not shown). Moreover, this migration defect could already be observed as early as the gastrula stage (Fig. 6E,F,E′,F′). These findings suggest that the defects in the anterior migration of the prechordal plate that are evident in the MZ *hdf* (*fgfr1*) mutant represent the primary cause of the anterior head malformation in these embryos.

Fgfr1 is required for the anterior movement of the axial mesoderm but is dispensable for the dorsal convergence movement of the lateral mesoderm during gastrulation

We speculated that the defective migration of the prechordal plate in the MZ *hdf* (*fgfr1*) mutant could be due to a consequence of impaired cell movement during gastrulation, such as epiboly and convergent extension. We thus analyzed the process of epiboly in both the maternal (M) and MZ embryos. The movement of epiboly, which drives blastoderm cells vegetally, proceeds normally in the M mutant, and we thus used sibling M mutants as controls in our subsequent analysis. The speed of epiboly movement in the MZ mutant was also found to be normal until the stage at which approximately 70% of the yolk sac is covered with blastoderm cells, i.e. 70% epiboly (Fig. 7A,B,F,G). However, as

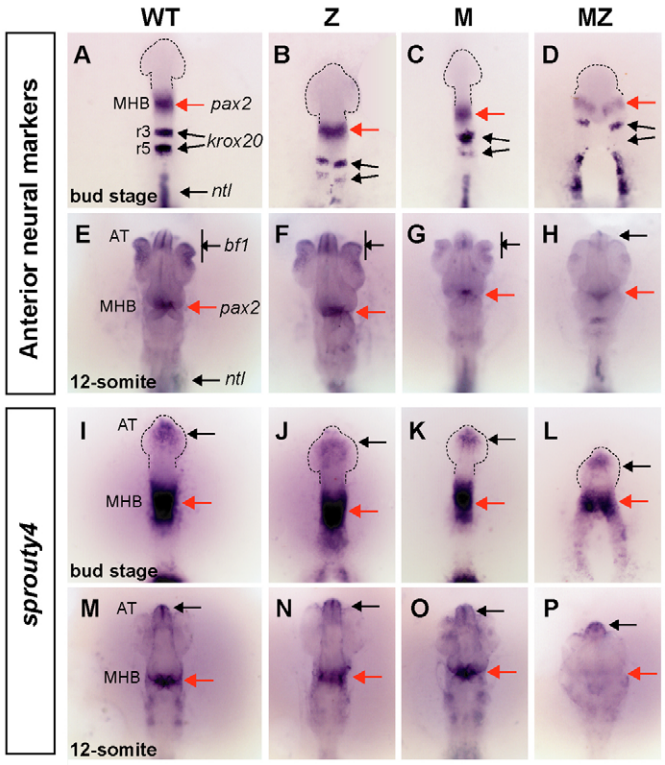

Fig. 5. The expression of anterior neural markers and *sprouty4* in the MZ *hdf* (*fgfr1*) medaka mutant. (**A-D**) Bud-stage (st. 18) embryos were hybridized with *pax2*, *krox20* and *ntl* probes. (**E-H**) Twelve-somite-stage (st. 23) embryos were hybridized with *bf1*, *pax2*, *krox20* and *ntl* probes. (**I-P**) Bud-stage (st. 18, I-L) and 12-somite-stage (st. 23, M-P) embryos were hybridized with a *sprouty4* probe. The anterior is at the top. The genotypes of the embryos are indicated on the top of each column of panels. Note that the expression levels of *bf1* at anterior telencephalon (black arrow in H), *pax2* at MHB (red arrow in H) and *sprouty4* at MHB (red arrow in P) are reduced in the MZ embryos at the 12-somite stage. AT, anterior telencephalon; M; maternal; MHB, midbrain-hindbrain boundary; MZ; maternal zygotic mutants; r3, rhombomere 3; r5, rhombomere 5; WT; wild type; Z, zygotic.

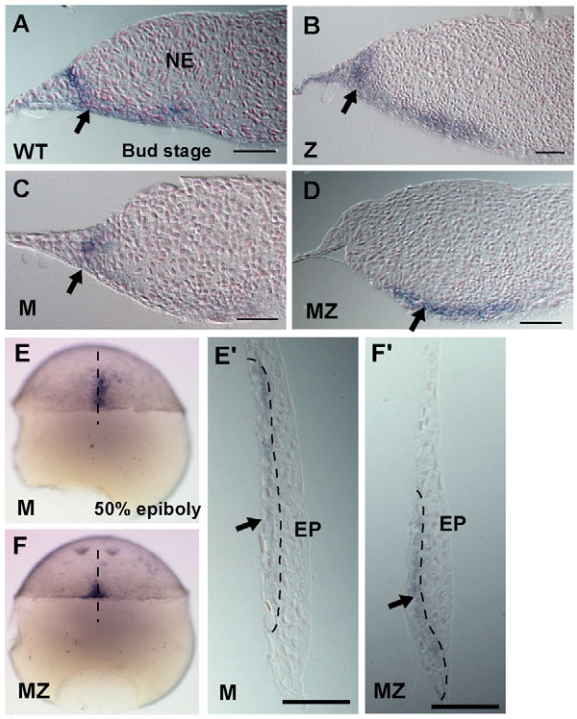

Fig. 6. Impaired development of the prechordal plate in the MZ *hdf* (*fgfr1*) medaka mutant. (**A-D**) Sagittal sections of the bud-stage (st. 18) embryos hybridized with a *gooescoid* (*gsc*) probe that stains the prechordal plate. Anterior head region (anterior to the left) is shown. Arrows indicate the expression domain of *gsc* (i.e. the prechordal plate) underlying the neural epithelium. Note that in the MZ embryo (D), the expression domain of *gsc* does not cover the entire anterior head region but is prematurely terminated. (**E**,**F**) Early migration of the prechordal plate at 50% epiboly (st 15). Dorsal views of maternal (E) and MZ (F) embryos stained with a *gsc* probe. (**E′**,**F′**) Sagittal sections through the dorsal midline of the embryos shown in E and F. Dashed lines in E′,F′ represent the border between the epiblast (EP, the future neural epithelium) and the migrating axial mesoderm (arrows). Scale bars: 100 μm in A-D; 50 μm in E′,F′. M; maternal; MZ; maternal zygotic *fgfr1* mutants; NE, neural epithelium; WT; wild type; Z, zygotic.

epiboly proceeded further, the extension of the embryonic midline tissues in the MZ *hdf* mutant was observed to become severely retarded, whereas the lateral and ventral margins moved vegetally at a normal speed, resulting in an abnormal V-shaped margin centered by the midline (Fig. 7C,D,H,I). Importantly, the epiboly of the MZ mutant completed with the same timing as the M mutant, leaving the axial margin arrested halfway along the animal-vegetal axis (Fig. 7E,J). These findings indicate that epiboly movement itself is normal in the MZ mutant embryo, with the exception of the axial region.

We next performed cell-tracing experiments using 4,5-dimethoxy-2-nitrobenzyl (DMNB)-caged fluorescein dextran (Fig. 7K-R). Again, we used sibling M mutants as the controls. Caged fluorescein was injected into one-cell stage M or MZ mutant embryos. To then monitor the anterior movement of the axial mesoderm, cells in the embryonic shield were marked by UV-mediated uncaging at the shield stage (Fig. 7K), and their locations were traced during gastrulation. In the M mutant, the marked cells were found to distribute in the dorsal axial hypoblast along the entire length of the anteroposterior axis at 6 hours after labeling [Fig. 7L,Q; (length of axial extension of labeled cells)/(length of yolk sac diameter)=0.55±0.05, n=7]. By contrast, the anterior movement of the marked cells in the MZ mutant was severely perturbed, resulting in a shortened axial mesoderm (Fig. 7M,Q; the ratio was 0.26±0.08, n=5, P=0.0002).

To trace the dorsal convergence movements in these embryos, we marked cells in the lateral blastoderm margin, at 90° from the dorsal embryonic shield, at the shield stage (Fig. 7N). During gastrulation, these marked mesoderm cells moved dorsally and anteriorly (white arrows in Fig. 7O,P), whereas those in the enveloping layer remained at the original angle and exhibited anterior expansion toward the animal pole (yellow arrows in Fig. 7O,P). Unexpectedly, labeled lateral cells in the MZ mutant also underwent normal convergence. This was confirmed by timecourse data obtained at the 6 hour (70% epiboly) and 12 hour (100% epiboly, st. 19) timepoints after labeling (Fig. 7R). These data thus indicate that Fgfr1-mediated signaling is specifically required for the expansion of the axial mesoderm along the anteroposterior axis, but is not required for the convergence movement of the lateral mesoderm.

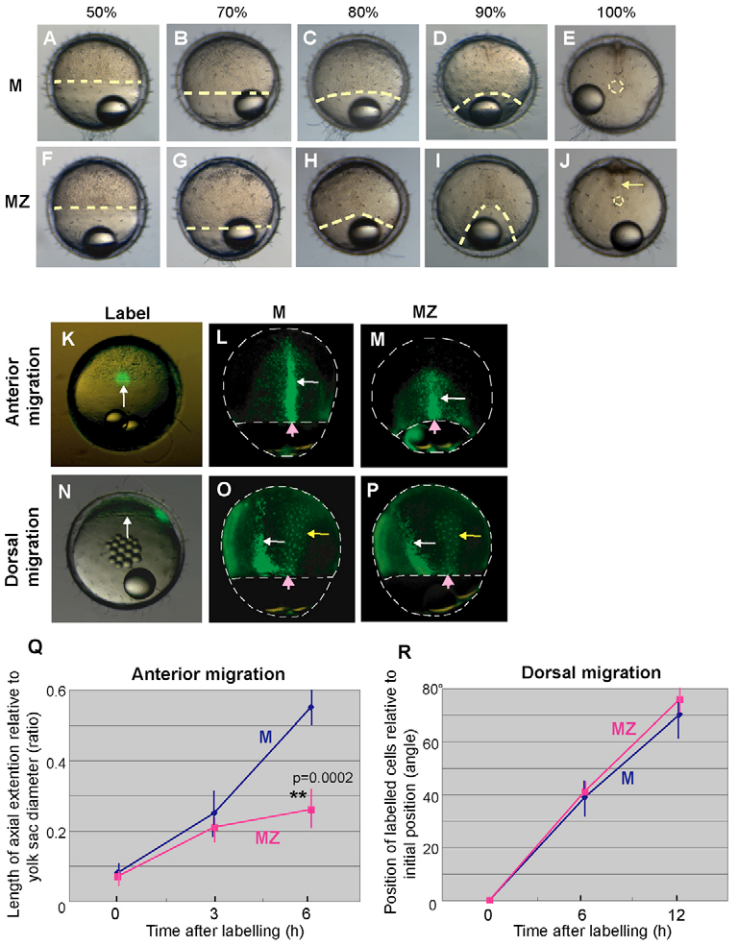

Fig. 7. Gastrulation movement in the MZ *hdf* (*fgfr1*) medaka mutant embryo. (**A-J**) Epiboly movement in the M (A-E) and MZ (F-J) mutants; the same embryo is shown at all stages in both cases. Dorsal views (animal pole is up) (A,B,F,G). Dorsal-vegetal views (C,D,H,I). Vegetal views (E,J). Dashed lines indicate the border between the blastoderm and the yolk sac. The arrow in J shows a narrow gap between the lateral marginal cells. Note that completion of epiboly in the MZ mutant occurs at the same time as in the M mutant except in the midline region (E,J). (**K-R**) Movement of the axial and lateral mesoderm cells of the MZ *hdf* (*fgfr1*) mutant. Axial (K) or lateral (N) mesoderm cells were labeled via the UV-mediated uncaging of DMNB-caged fluorescein-dextran at the shield stage (st. 14), and traced for anterior migration (L,M) and dorsal migration (O,P), respectively. Arrows in K and N indicate the embryonic shield. The white arrows in L,M,O,P indicate locations of the labeled mesoderm cells at 6 hours after uncaging. The yellow arrows in O,P highlight the enveloping layer. Initial labeling positions are represented by pink arrows in L,M,O,P. (Q,R) Graphs comparing the migration of labeled cells in M (blue) and MZ (red) mutant embryos. Anterior migration (Q) was quantified by the ratio of the length of labeled cells relative to the yolk sac diameter. Dorsal migration (R) was quantified by the angle between the central position of the labeled cells relative to their initial position at the shield stage.

Fgfr1 acts in a cell-autonomous manner during prechordal plate progenitor migration

As *fgfr1* is broadly expressed until mid-gastrulation, we postulated that the effects of Fgfr1 upon axial cells could be non-cell-autonomous. To address this possibility, we transplanted prechordal plate precursor cells (a group of cells that first involute in the dorsal margin) obtained from MZ mutants into wild-type embryos at the shield stage and vice versa (Fig. 8A). In this series of experiments, we used MZ embryos obtained from female medaka whose germ cells had been eliminated by the morpholino knockdown of *cxcr4* (Kurokawa et al., 2006). At the bud stage (90% epiboly, st. 18), the migratory ability of the precursor cells was assayed by the position of their anterior limits (Fig. 8A). In most control transplants (in which both the donor and host embryos were wild type), the transplanted cells moved and distributed along the entire axial tissue, including the anterior of the prechordal plate (transplants that showed successful migration: 14/15) (Fig. 8B,E). However, when the MZ mutant cells were transplanted into wild-type embryos, the anterior limit of the migrating cells tended to shift posteriorly compared with the control transplants (successful migration: 3/16) (Fig. 8C,F). Wild-type cells, by contrast, migrated almost normally to the most anterior region in the MZ-mutant background (successful migration: 12/12) (Fig. 8D,G). Histological sections confirmed that the transplanted cells had distributed in the prechordal plate (Fig. 8H-S). These results clearly show that Fgfr1 acts cell-autonomously in prechordal plate precursor cells during their anterior migration.

Interestingly, we further found that transplanted wild-type cells partially rescued the phenotypes of the anterior head structures in the MZ *fgfr1* mutant. Whereas over 95% (40/42) of the non-operated MZ mutants exhibited cyclopia, the phenotype of MZ mutants harboring transplanted wild-type cells was much improved, with only 2 out of 12 displaying cyclopic features, and the remaining 10 showing two eyes separated by almost normal distances. These observations further support our contention that the defective anterior migration of the prechordal plate is a primary cause of the severely affected head structures in the MZ *fgfr1* mutant.

DISCUSSION

Germline replacement using hybrid fish

In our present study, we demonstrate functional germ-cell replacement in the medaka that takes advantage of interspecific hybrid sterility so that female hybrids between Japanese and Hainan medaka strains can be used as surrogate mothers. Germline replacement was first reported in vertebrates by A. Schier and colleagues, who used zebrafish homozygous mutant donors (Ciruna et al., 2002). In their report, the elimination of the host germline cells was achieved by morpholino knockdown of *dead end*, an essential gene required for PGC development, before the donor PGCs were transplanted. In our current method, we avoid this step by taking advantage of interspecific hybrid sterility in the medaka. We have compared the embryonic phenotypes of the MZ *hdf* embryos obtained using interspecific hybrids and also that had derived from *cxcr4*-MO-injected parents, and found no significant differences

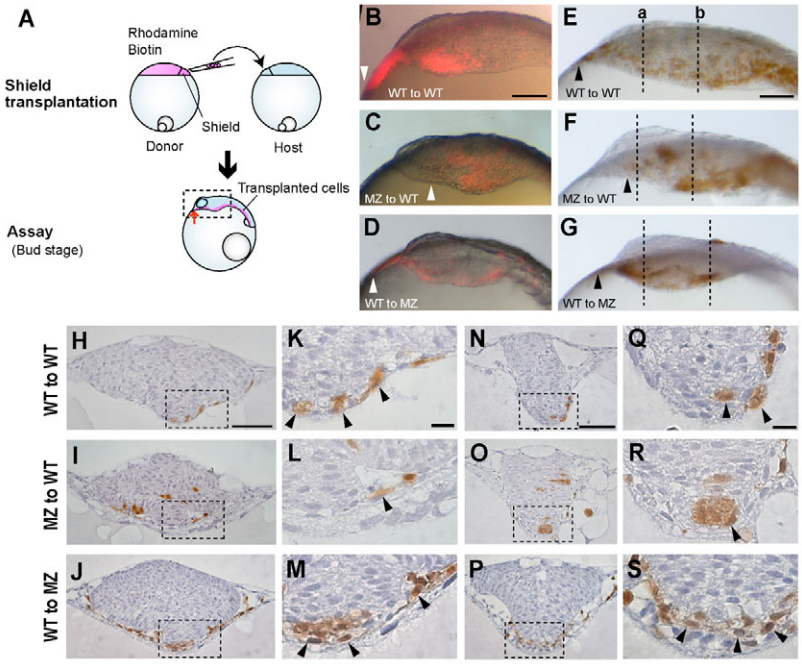

Fig. 8. Cell-autonomous role of Fgfr1 during anterior migration of axial mesoderm cells in the medaka. (**A**) Schematic illustration of the shield transplantation experiment. Donor cells were labeled by both rhodamine-dextran and biotin-dextran. The migrating ability of the transplanted cells was then assayed at the bud stage (st. 18) by assessing the position of the anterior limits of the labeled cells (indicated by the arrow). (**B-G**) Lateral views of the representative transplanted embryos. Anterior is to the left. Rhodamine-labeled cells in the live embryos (B-D) or biotin-labeled cells in the fixed embryos (E-G) contribute to the axial mesoderm in the host embryos. (B,E) Donor, wild type; host, wild type. Transplanted cells reach the most anterior mesoderm region. (C,F) Donor, MZ mutant; host, wild type. The anterior limit of the migrating cells shifts posteriorly compared with the control transplant in B,E. (D,G) Donor, wild type; host, MZ mutant. The anterior limit of the transplanted cells is located at the most anterior region. Arrowheads indicate the positions of the anterior limits of the migratory cells. (**H-S**) Cross sections of the anterior neural regions. (H-M) Cross sections at the level of the eye vesicle region (indicated by the dashed lines, a, in E-G). (N-S) Cross sections at the level of the hindbrain region (indicated by the dashed lines, b, in E-G). (K-M,Q-S) Higher magnification of the dashed boxes shown in H-J and N-P, respectively. Biotin-labeled cells contribute to the prechordal mesoderm in the host embryos (arrowheads in K-M and Q-S). Scale bars: 100 μm in B,E; 50 μm in H,N; 10 μm in K,Q.

between them. Hence both approaches produce comparable results in the medaka, and we contend that our novel procedure using interspecific hybrids is a simpler and faster method. Indeed, the resulting hybrid offspring also exhibit a faster growth rate than normal, as a consequence of which the transplanted hybrid females usually begin laying eggs at 5 to 6 weeks of age.

Fgfr1-mediated signaling is dispensable for mesoderm induction

In lower vertebrates, the functional analysis of *fgfr1* has mainly been performed by injections of mRNA encoding a dominant negative form of Fgfr1 (XFD). One of the main conclusions to result from these experiments is that blocking the function of Fgfr1 in early stage *Xenopus* and zebrafish embryos inhibits mesoderm induction, leading to truncation of the anteroposterior axis (Amaya et al., 1991; Amaya et al., 1993; Carl and Wittbrodt, 1999; Griffin et al., 1995; Launay et al., 1996). However, in the *Fgfr1*-mutant mouse, initial mesoderm formation occurs normally (Deng et al., 1994; Yamaguchi et al., 1994). This discrepancy could be due to the fact that XFD interference has no specific preference for any type of Fgfr (Ueno et al., 1992), or may be due to the maternal contribution of Fgfr1 in mice, where maternal effects are thought to be limited. However, in the MZ medaka mutant for *fgfr1*, the early mesodermal markers *ntl* and *fgf8* are initially activated in the blastoderm margin, indicating that Fgfr1-mediated signaling is dispensable for mesoderm induction in fish. Fgf signaling, mediated by receptors other than Fgfr1, could conceivably compensate and participate in this process, but this is not very likely for a number of reasons. First, *ntl* is activated in MZ embryos in the absence of the induction of *sprouty4*, a downstream target of Fgf signaling (Minowada et al., 1999). More importantly, *ntl* expression persists in wild-type embryos treated with the chemical inhibitor SU5402, which is known to block nearly all types of Fgfr. As mesoderm formation is also severely impaired in mouse and zebrafish mutants for Nodal signaling (Gritsman et al., 1999; Zhou et al., 1993), this pathway may play an essential role in mesoderm induction in these organisms.

The MZ *hdf* (*fgfr1*) mutant reveals an early and essential role for Fgfr1 in prechordal plate migration

The MZ *hdf* (*fgfr1*) mutant displays severe anterior neural defects that are never observed in its zygotic counterpart. This was found to be attributable to a defective migration of the prechordal plate. In addition to the organizing centers within the neural ectoderm, the underlying prechordal plate plays a crucial role in anterior neural patterning, which secretes signaling molecules such as Shh, Dickkoff1 and the Fgfs (Niehrs et al., 2001; Placzek and Briscoe, 2005; Shinya et al., 2000). The role of the prechordal plate in neural patterning has been clearly shown in zebrafish *one-eyed pinhead* (*oep*) mutants in which Nodal signaling is zygotically blocked. In this mutant, the prechordal plate fails to form, and the anterior head structures are severely affected (Schier et al., 1997; Shinya et al., 2000). This phenotype is

very similar to the one we observe in the medaka MZ mutant for *hdf* (*fgfr1*). However, expression and cell-tracing analyses of these embryos have revealed that unlike the zebrafish *oep* mutant, the medaka MZ *fgfr1* mutant develops a (*gsc*-positive) prechordal plate but its anterior migration, underneath the neural region, fails to complete, leading to an arrest somewhere between the anterior neural ridge and the MHB. As maternally provided proteins do not persist for long after fertilization, until mid-gastrulation at most (Yokoi et al., 2007), they should function before gastrulation has completed. Consistently, the defect in axial elongation, the earliest phenotype of the MZ embryo, becomes detectable at the gastrula stage.

Interestingly, in spite of the early roles of *fgfr1*, both the maternal and zygotic medaka mutants for *hdf* (*fgfr1*) in our present study develop a normal anterior head, and this indicates that either maternally or zygotically derived Fgfr1 is sufficient for normal migration of the prechordal plate. Hence, the production of MZ mutants was the only way to uncover this early function of *fgfr1* in lower vertebrates in which, unlike the mouse, maternally supplied materials sometimes play an essential role in early development.

There is now increasing evidence for the role of Fgf signaling in cell movement or migration during early development in vertebrates. Examples of this include the overexpression of *Xsprouty2*, a negative regulator of Fgf signaling (Nutt et al., 2001), and the knockdowns of neurotrophin receptor homolog (NRH) and ankyrin repeat domain protein 5 (Anr5), both Fgf downstream targets (Chung et al., 2005; Chung et al., 2007), which result in the inhibition of cell movement during convergent extension. In addition, chimeric analyses of the *Fgfr1*-knockout mouse have shown that these mutant cells fail to move away from the primitive streak (Ciruna and Rossant, 2001; Ciruna et al., 1997). Our present analyses of MZ *fgfr1* mutant medaka embryos further specify the role of Fgfr1 in embryonic cell movement using genetic approaches and have demonstrated the specific requirement for this factor during cell migration in the axial mesoderm. The differentiation of the axial mesoderm must also be impaired from the beginning, but judging from *ntl* and *gsc* expression, the initial differentiation of this structure does take place in the MZ mutant. Overall, the defective cell migration is most evident in the prechordal plate, the precursors of which require the highest levels of cell migration in order that the cells travel the considerable distance from the margin to eventually underlie the anterior of the neural tube.

Our current transplantation study also provides evidence that Fgfr1-mediated signaling acts in a cell-autonomous manner. Thus, Fgfr1-mediated signaling appears to directly control the migratory activity of axial cells in fish. In medaka, Fgf8 has been suggested to be a main ligand for Fgfr1 during early development because of the phenotypic similarity between zygotic *hdf* mutant and *fgf8* morphant (Yokoi et al., 2007). This could be the case for prechordal plate migration, because *fgf8* expresses in the early mesodermal lineage (H.Y., unpublished). However, it remains to be elucidated whether this ligand directs a migratory pathway or simply activates migratory behavior. Recent work demonstrated that prechordal plate migration is directed by platelet derived growth factor (PDGF) and its receptor (PDGFR) in *Xenopus* and zebrafish (Liu et al., 2002; Nagel et al., 2004). It is thus possible that Fgfr1-mediated signaling cooperates with PDGF signaling in anterior migration of axial mesodermal cells.

In conclusion, we have generated an MZ *hdf* (*fgfr1*) mutant in the medaka and have conducted phenotypic analysis, which has revealed the early cell-autonomous role of this gene during axial migration. Considering the advantages of using fish model systems in developmental studies, this *hdf* mutant could prove to be a valuable model with which to analyze the precise role of *fgfr1*-mediated signaling in early vertebrate development.

We thank Yasuko Ozawa and Shizuko Takada for their excellent care of the fish used in this study. We also thank Dr Minoru Tanaka for giving *cxcr4* morpholino oligonucleotides. This work was supported in part by Grants-in-Aid for Scientific Research Priority Area Genome Science and the Organized Research Combination System from the Ministry of Education, Culture, Sports, Science and Technology of Japan.

References

Amaya, E., Musci, T. J. and Kirschner, M. W. (1991). Expression of a dominant negative mutant of the FGF receptor disrupts mesoderm formation in Xenopus embryos. *Cell* **66**, 257-270.

Amaya, E., Stein, P. A., Musci, T. J. and Kirschner, M. W. (1993). FGF signalling in the early specification of mesoderm in Xenopus. *Development* **118**, 477-487.

Bottcher, R. T. and Niehrs, C. (2005). Fibroblast growth factor signaling during early vertebrate development. *Endocr. Rev.* **26**, 63-77.

Carl, M. and Wittbrodt, J. (1999). Graded interference with FGF signalling reveals its dorsoventral asymmetry at the mid-hindbrain boundary. *Development* **126**, 5659-5667.

Chung, H. A., Hyodo-Miura, J., Nagamune, T. and Ueno, N. (2005). FGF signal regulates gastrulation cell movements and morphology through its target NRH. *Dev. Biol.* **282**, 95-110.

Chung, H. A., Yamamoto, T. S. and Ueno, N. (2007). ANR5, an FGF target gene product, regulates gastrulation in Xenopus. *Curr. Biol.* **17**, 932-939.

Ciruna, B. and Rossant, J. (2001). FGF signaling regulates mesoderm cell fate specification and morphogenetic movement at the primitive streak. *Dev. Cell* **1**, 37-49.

Ciruna, B. G., Schwartz, L., Harpal, K., Yamaguchi, T. P. and Rossant, J. (1997). Chimeric analysis of fibroblast growth factor receptor-1 (Fgfr1) function: a role for FGFR1 in morphogenetic movement through the primitive streak. *Development* **124**, 2829-2841.

Ciruna, B., Weidinger, G., Knaut, H., Thisse, B., Thisse, C., Raz, E. and Schier, A. F. (2002). Production of maternal-zygotic mutant zebrafish by germ-line replacement. *Proc. Natl. Acad. Sci. USA* **99**, 14919-14924.

Deng, C. X., Wynshaw-Boris, A., Shen, M. M., Daugherty, C., Ornitz, D. M. and Leder, P. (1994). Murine FGFR-1 is required for early postimplantation growth and axial organization. *Genes Dev.* **8**, 3045-3057.

Fekany, K., Yamanaka, Y., Leung, T., Sirotkin, H. I., Topczewski, J., Gates, M. A., Hibi, M., Renucci, A., Stemple, D., Radbill, A. et al. (1999). The zebrafish bozozok locus encodes Dharma, a homeodomain protein essential for induction of gastrula organizer and dorsoanterior embryonic structures. *Development* **126**, 1427-1438.

Fukamachi, S., Shimada, A. and Shima, A. (2001). Mutations in the gene encoding B, a novel transporter protein, reduce melanin content in medaka. *Nat. Genet.* **28**, 381-385.

Furutani-Seiki, M., Sasado, T., Morinaga, C., Suwa, H., Niwa, K., Yoda, H., Deguchi, T., Hirose, Y., Yasuoka, A., Henrich, T. et al. (2004). A systematic genome-wide screen for mutations affecting organogenesis in Medaka, Oryzias latipes. *Mech. Dev.* **121**, 647-658.

Griffin, K., Patient, R. and Holder, N. (1995). Analysis of FGF function in normal and no tail zebrafish embryos reveals separate mechanisms for formation of the trunk and the tail. *Development* **121**, 2983-2994.

Gritsman, K., Zhang, J., Cheng, S., Heckscher, E., Talbot, W. S. and Schier, A. F. (1999). The EGF-CFC protein one-eyed pinhead is essential for nodal signaling. *Cell* **97**, 121-132.

Hamaguchi, S. and Sakaizumi, M. (1992). Sexually differentiated mechanisms of sterility in interspecific hybrids between Oryzias latipes and O. curvinotus. *J. Exp. Zool.* **263**, 323-329.

Ishikawa, Y. (2000). Medakafish as a model system for vertebrate developmental genetics. *BioEssays* **22**, 487-495.

Kasahara, M., Naruse, K., Sasaki, S., Nakatani, Y., Qu, W., Ahsan, B., Yamada, T., Nagayasu, Y., Doi, K., Kasai, Y. et al. (2007). The medaka draft genome and insights into vertebrate genome evolution. *Nature* **447**, 714-719.

Kimura, T., Jindo, T., Narita, T., Naruse, K., Kobayashi, D., Shin, I. T., Kitagawa, T., Sakaguchi, T., Mitani, H., Shima, A. et al. (2004). Large-scale isolation of ESTs from medaka embryos and its application to medaka developmental genetics. *Mech. Dev.* **121**, 915-932.

Kurokawa, H., Aoki, Y., Nakamura, S., Ebe, Y., Kobayashi, D. and Tanaka, M. (2006). Time-lapse analysis reveals different modes of primordial germ cell migration in the medaka Oryzias latipes. *Dev. Growth Differ.* **48**, 209-221.

Launay, C., Fromentoux, V., Shi, D. L. and Boucaut, J. C. (1996). A truncated FGF receptor blocks neural induction by endogenous Xenopus inducers. *Development* **122**, 869-880.

Liu, L., Chong, S. W., Balasubramaniyan, N. V., Korzh, V. and Ge, R. (2002). Platelet-derived growth factor receptor alpha (pdgfr-alpha) gene in zebrafish embryonic development. *Mech. Dev.* **116**, 227-230.

Minowada, G., Jarvis, L. A., Chi, C. L., Neubuser, A., Sun, X., Hacohen, N., Krasnow, M. A. and Martin, G. R. (1999). Vertebrate Sprouty genes are induced by FGF signaling and can cause chondrodysplasia when overexpressed. *Development* **126**, 4465-4475.
Mohammadi, M., McMahon, G., Sun, L., Tang, C., Hirth, P., Yeh, B. K., Hubbard, S. R. and Schlessinger, J. (1997). Structures of the tyrosine kinase domain of fibroblast growth factor receptor in complex with inhibitors. *Science* **276**, 955-960.
Nagel, M., Tahinci, E., Symes, K. and Winklbauer, R. (2004). Guidance of mesoderm cell migration in the Xenopus gastrula requires PDGF signaling. *Development* **131**, 2727-2736.
Naruse, K., Tanaka, M., Mita, K., Shima, A., Postlethwait, J. and Mitani, H. (2004). A medaka gene map: the trace of ancestral vertebrate proto-chromosomes revealed by comparative gene mapping. *Genome Res*. **14**, 820-828.
Niehrs, C., Kazanskaya, O., Wu, W. and Glinka, A. (2001). Dickkopf1 and the Spemann-Mangold head organizer. *Int. J. Dev. Biol*. **45**, 237-240.
Nutt, S. L., Dingwell, K. S., Holt, C. E. and Amaya, E. (2001). Xenopus Sprouty2 inhibits FGF-mediated gastrulation movements but does not affect mesoderm induction and patterning. *Genes Dev*. **15**, 1152-1166.
Placzek, M. and Briscoe, J. (2005). The floor plate: multiple cells, multiple signals. *Nat. Rev. Neurosci*. **6**, 230-240.
Schier, A. F., Neuhauss, S. C., Helde, K. A., Talbot, W. S. and Driever, W. (1997). The one-eyed pinhead gene functions in mesoderm and endoderm formation in zebrafish and interacts with no tail. *Development* **124**, 327-342.
Shinya, M., Eschbach, C., Clark, M., Lehrach, H. and Furutani-Seiki, M. (2000). Zebrafish Dkk1, induced by the pre-MBT Wnt signaling, is secreted from the prechordal plate and patterns the anterior neural plate. *Mech. Dev*. **98**, 3-17.
Thisse, B. and Thisse, C. (2005). Functions and regulations of fibroblast growth factor signaling during embryonic development. *Dev. Biol*. **287**, 390-402.
Ueno, H., Gunn, M., Dell, K., Tseng, A., Jr and Williams, L. (1992). A truncated form of fibroblast growth factor receptor 1 inhibits signal transduction by multiple types of fibroblast growth factor receptor. *J. Biol. Chem*. **267**, 1470-1476.
Wittbrodt, J., Shima, A. and Schartl, M. (2002). Medaka-a model organism from the far East. *Nat. Rev. Genet*. **3**, 53-64.
Yamaguchi, T. P., Harpal, K., Henkemeyer, M. and Rossant, J. (1994). fgfr-1 is required for embryonic growth and mesodermal patterning during mouse gastrulation. *Genes Dev*. **8**, 3032-3044.
Yamamoto, T. (1956). The physiology of fertilization in the medaka (Oryzias latipes). *Exp. Cell Res*. **10**, 387-393.
Yasumasu, S., Iuchi, I. and Yamagami, K. (1989). Purification and partial characterization of high choriolytic enzyme (HCE), a component of the hatching enzyme of the teleost, Oryzias latipes. *J. Biochem*. **105**, 204-211.
Yokoi, H., Shimada, A., Carl, M., Takashima, S., Kobayashi, D., Narita, T., Jindo, T., Kimura, T., Kitagawa, T., Kage, T. et al. (2007). Mutant analyses reveal different functions of fgfr1 in medaka and zebrafish despite conserved ligand-receptor relationships. *Dev. Biol*. **304**, 326-337.
Zhou, X., Sasaki, H., Lowe, L., Hogan, B. L. and Kuehn, M. R. (1993). Nodal is a novel TGF-beta-like gene expressed in the mouse node during gastrulation. *Nature* **361**, 543-547.